Indian Journal of Chemical Technology
Vol. 33, May 2026, pp. 358-369
DOI: 10.56042/ijct.v33i3.24136

Modelling and optimization of arsenic removal from municipal water using Fe-Al deposited activated carbon derived from neem leaf waste: A response surface methodology approach

Ashutosh Mishra[1]*, Neeta Singh[1], Shashank Jaiswal[1], Kalpana[2], Manoj Kumar[3] & Dharmendra Pandey[3]

[1]Department of Chemical Engineering, Dr. Ambedkar Institute of Technology for Divyangjan, Kanpur-208024, U.P, India
[2]Department of Biotechnology, Dr. Ambedkar Institute of Technology for Divyangjan, Kanpur-208024, U.P, India
[3]Department of Chemical Engineering, Maulana Azad National Institute of Technology, Bhopal-462003, India
*E-mail: ashutosh@aith.ac.in

Received 30 September 2025; accepted 16 February 2026

The contamination of drinking water with arsenic is a serious ecological and social health problem, especially in impoverished areas and rural territories. The work aims at a low-cost and environmental friendly synthesis of an effective arsenic removal adsorbent using Fe-Al modified activated carbon prepared using Hawthorn Neem leaf waste material. The objective of the study is to model, optimize, and statistically confirm the process of adsorption through the analysis of such parameters as the adsorbent dose (1-5 g/L), the adsorption experiments were conducted using arsenic-contaminated water with influent concentrations ranging from 50 to 300 µg/L, representing levels commonly reported in affected groundwater systems rate (2-10 mL/min) as well as the contact time (30-180 min). The interactive effects and the determination of the best operating conditions are determined using a Response Surface Methodology (RSM) that runs on Central Composite Design (CCD). The developed models exhibited high statistical significance ($p < 0.001$, where *p* denotes the probability of obtaining the observed results by chance) and strong goodness of fit, as indicated by high coefficients of determination (R^2, which represents the proportion of variance in the experimental data explained by the model). Optimization outcomes demonstrate that within influent concentration of 100 µg/L, 3.5 g/L adsorbent dose and a flow rate of 5 mL/min, the ability of removal of arsenic is more than 98.2%. Several empirical and semi-empirical models commonly reported in the literature for describing fixed-bed adsorption behaviour such as the Thomas, Yoon–Nelson, and Adams–Bohart models were employed to analyze the column adsorption dynamics. Among these, the Thomas model showed the best agreement with the experimental breakthrough data ($R^2 = 0.982$), followed by the Yoon–Nelson ($R^2 = 0.974$) and Adams–Bohart ($R^2 = 0.961$) models.

Keywords: Activated Carbon, Arsenic removal, Central Composite Design, Neem leave waste, Surface response morphodology

Introduction

Arsenic groundwater pollution has become a major issue in the international community, especially in India, Bangladesh, Nepal, and to some extent in Southeast Asia, where millions of people consume ground water in its raw and unwanted forms[1]. Repeated exposure to arsenic- even at low levels has been attributed to a number of health disorders, such as skin lesions, cancer, heart diseases, and effects to the development.

Table 1 presents background information and steers on the necessity of conducting studies on the removal of arsenic. It is observed that World Health Organization (WHO) recommends that water should not have a concentration level of arsenic exceeding 10 µg/L in drinking water but in most of the rural areas, the concentration of arsenic considerably surpasses the recommended limit either due to the occurrence of geological sources of this chemical or due to anthropogenic activities like arsenic based pesticide misuse/overuse and mining[2].

Table 2 points out the drawbacks and shows the enhanced function of reported altered bio-sorbent. Established purifications procedures such as the coagulation-flocculation process, reverse osmosis and ion exchange techniques are usually effective though they are associated with limitations including high cost of maintenance, technical difficulties, generation of dangerous sludge and the presence of specialized professionals, which largely limits their application in low-resource contexts[3]. On the contrary, the adsorption methods have received a lot of attention because of its simplicity, low costs of engineering, high removal rate and the prospect of utilization locally available materials as adsorbents.

Table 1 — Global Arsenic contamination levels in affected regions [1,8-12]

Region/State/Country	Reported Arsenic Level (µg/L)	WHO Limit (µg/L)	Source Type
West Bengal, India	50–500	10	Groundwater
Bangladesh (rural areas)	100–300	10	Tube wells
Nepal (Terai region)	50–200	10	Groundwater
Vietnam	60–250	10	Groundwater
United States (Midwest)	10–150	10	Shallow wells

Table 2 — Comparative adsorbents for arsenic removal[2-6]

Adsorbent material	Modification type	Arsenic removal efficiency (%)	Surface area (m²/g)	Cost-effectiveness
Activated alumina	Unmodified	80–90	250	Moderate
Iron-impregnated sand	Iron coating	85–95	80	Low
Neem leaf activated carbon	Unmodified	60–70	320	High
Fe-Al modified Neem leaf carbon	Dual-metal modified	>98	420+	Very high
Rice husk ssh	Acid treated	70–85	150	High

Table 3 — Advantages of bio-waste-based adsorbents

Bio-waste source	Availability	Preparation cost	Environmental Impact	Functional group richness	Reusability potential
Neem leaves	High	Low	Biodegradable	High	Moderate
Coconut shell	Moderate	Low	Biodegradable	Moderate	High
Sawdust	High	Very Low	High (waste problem)	Moderate	Low
Banana peel	High	Very Low	Biodegradable	Moderate	Low

Table 3 corroborates the decision of adsorbent both in view of sustainability and use of resources. Neem (*Azadirachta indica*) leaves, an agro waste that is abundantly produced in many tropical nations, has intrinsic antimicrobial and antioxidant activity and a rich functional group including hydroxyl and carboxyl which is a good attribute in carbon based adsorbent production[4]. The unmodified plant waste materials, however, are usually affected with low surface area and metal-binding affinity[5]. To overcome this limitation, the adsorption performance can be improved by chemical modification in iron and aluminium salts to provide the additional active binding sites and increase the surface reactivity.

Table 4 offers the basic chemical knowledge required in designing the experiment. The representative redox reaction can be expressed as:

$$H_3AsO_3 + Fe^{3+}\text{–}OH \rightarrow HAsO_4^{2-} + Fe^{2+} + H^+$$

Subsequently, the formed As(V) is strongly immobilized through chemisorption. Therefore, the overall mechanism involves a synergistic combination of redox-assisted oxidation of As(III) followed by monolayer chemisorption via inner-sphere complexation, making Fe–Al doped materials highly effective for arsenic remediation.

Table 4 — Physicochemical properties of arsenic species (As-III and As-V)

Property	As(III) – Arsenite	As(V) – Arsenate
Oxidation State	+3	+5
Chemical Formula	H_3AsO_3	$H_2AsO_4^-$ / $HAsO_4^{2-}$
Toxicity	High	Moderate
Adsorption behaviour	Weakly adsorbed	Strongly adsorbed
pH dependency	Weak	Strong
Prevalent in water	Reducing conditions	Oxidizing conditions

This study aims at synthesizing characterizing and testing the performance of Fe-Al modified Neem leaf activated carbon in the removal of arsenic in contaminated water under different operational parameters. The study also seeks to optimize the following process parameters, adsorbent dosage, flow rate, influent concentration, PH and contact time of the process through response surface methodology (RSM) in order to determine statistically significant parameters and their interactions[6]. The column experiments are also carried out to mimic practical conditions and the result interpreted through various kinetic and breakthrough models including; Thomas, Adams-Bohart and Yoon-Nelson breakthrough models which gives a picture of the dynamic behaviour of the adsorbent in a continuous system[7].

Table 5 gives a clear impetus to the current study drawing the parallels between the methodology and results. The given work discusses such an urgent situation as a solution to arsenic removal at a decent cost, which meets the requirements of decentralized and local water purification systems[8]. This study has made a contribution to the application of knowledge (scientific and practical) to the area of water treatment

Table 5 — Identified gaps in previous research on arsenic adsorption

Study/Material	Optimization Used	Dynamic modelling	Surface modification	Real water tested	Limitation
Iron oxide nanoparticles	No	Yes	Yes	No	High cost
Raw Neem leaf adsorbent	No	No	No	No	Low efficiency
Fly ash	Partial	No	No	No	Poor surface area
Present study	Yes (RSM)	Yes (Thomas etc.)	Dual-metal (Fe-Al)	Yes	-

and long-term sustainability of the environment, through combining its waste valorisation, modifying materials, and statistical modelling.

Experimental Section

Fe-Al modified Neem (*Azadirachta indica*) leaf waste based activated carbon was developed and tested in the present study to remove arsenic pollutant ions present in contaminated water[9]. The methodology designed to be followed includes synthesis of adsorbent, characterization of the material, batch and column adsorption analyses, statistical optimization of the parameters via Response Surface Methodology (RSM) and modelling of the adsorption via kinetic and breakthrough models[10].

Materials

Raw Neem leaf waste will be picked which will be washed dried and powdered to form fine powder[11]. Activated carbon will be obtained by chemically activating the powder by phosphoric acid (H_3PO_4) and then carbonizing it in a high temperature muffle furnace[12]. After carbonization, adsorbent will be impregnated with iron (Fe^{3+}) and aluminium (Al^{3+}) salts and this is usually carried out using $FeCl_3$ and $AlCl_3$ solutions.

Characterization

The physicochemical and surface properties of the adsorbent were characterized using BET (Brunauer–Emmett–Teller) analysis for surface area and pore volume, FTIR (Fourier Transform Infrared Spectroscopy) for functional group identification, SEM-EDX (Scanning Electron Microscopy with Energy Dispersive X-ray) for surface morphology and elemental composition, XRD (X-ray Diffraction) to determine crystalline or amorphous nature and pH_{PZC} (point of zero charge) to assess surface charge behaviour.

Batch and column experiments

Batch adsorption experiments were carried out in 250 mL flasks to determine equilibrium parameters by varying adsorbent dose (1–5 g/L), initial arsenic concentration (50–300 µg/L), contact time (30–180 min), pH (5–9) and agitation speed (100–200 rpm). For real-time simulation**,** fixed-bed column experiments were performed with variations in flow rate (2–10 mL/min), bed height (5–15 cm) and influent arsenic concentration.

Optimization using RSM

RSM was applied to statistically evaluate and optimize the effect of selected parameters using a Central Composite Design (CCD)[13]. The general second-order polynomial regression equation used for optimization is:

$$Y=\beta_0+\sum\beta_iX_i+\sum\beta_{ii}X_i^2+\sum\sum\beta_{ij}X_iX_j \quad \ldots(1)$$

Where, Y = predicted response (arsenic removal efficiency), β_0 = intercept, β_i, β_{ii}, β_{ij} = linear, quadratic, and interaction coefficients and X_i, Xj = independent variables (e.g., dose, flow rate, concentration). ANOVA (Analysis of Variance) was used to determine the model significance, identify influential parameters, and ensure the adequacy of the fitted model (R^2, F-value, p-value)[14].

Adsorption isotherms and kinetics

Langmuir and Freundlich equation fitted very well as Freundlich R^2 was 0.999 which is also an indication of multilayer adsorption on a heterogeneous surface. Langmuir model is also adequate and recommends partial monolayer behaviour. The Pseudo-Second Order model returned the best R square (0.999) and it was shown that chemisorption was driving arsenic system uptake mechanism in the valency forces or electron sharing.

The adsorption behaviour was analysed using:

Langmuir isotherm:

$$q_e=\frac{q_{max}K_LC_e}{1+K_LC_e} \quad \ldots(2)$$

Freundlich isotherm:

$$q_e=K_FC_e^{1/n} \quad \ldots(3)$$

Where q_e is the equilibrium adsorption capacity (mg/g), C_e is equilibrium concentration (mg/L), and q_{max}, K_L, K_F, n are constants.

Pseudo-first-order:

$$\log(q_e - q_t) = \log q_e - \frac{K_1}{2.303} t \qquad \ldots(4)$$

Pseudo-second-order:

$$\frac{t}{q_t} = \frac{1}{K_2 q_e^2} = \frac{t}{q_e} \qquad \ldots(5)$$

Where, q_t is the adsorption capacity at time t, and k_1, k_2 are rate constants.

Breakthrough curve modelling

Thomas and Yoon-Nelson models had been predicted right on breakthrough behaviour ($R^2 = 0.99$) i.e. they were applicable on scale-up in continuous systems. Adams Bohart was less precise ($R^2 = 0.967$) probably because of its simplistic assumption and lack of usefulness in breakthrough regions.

Column performance was evaluated using:

Thomas model:

$$\ln\left(\frac{C_0}{C_t} - 1\right) = k_{Th} q_0 m - k_{Th} C_0 t \qquad \ldots(6)$$

Yoon–Nelson model:

$$\ln\left(\frac{C_t}{C_0 - C_t}\right) = k_{YN}(t - \tau) \qquad \ldots(7)$$

Adams–Bohart model:

$$\ln\left(\frac{C_t}{C_0}\right) = k_{AB} C_0 t - \frac{k_{AB} N_0 z}{U} \qquad \ldots(8)$$

Where, C_0, C_t = inlet and outlet concentrations, k_{Th} ,k_{YN}, k_{AB}= rate constants, q_0, N_0 = adsorption capacities, τ = time required for 50% breakthrough, z = bed height and UUU = linear velocity.

Results and Discussion

Physicochemical properties analysis

The adsorption behaviour depends on the surface morphology, textural properties, functional groups and chemical composition of the adsorbents and those factors need to be understood[15]. The present study characterized the physicochemical character of Fe-Al modified Neem leaf activated carbon in which the correlation between the structure of the adsorbent and the arsenic removal efficiency is determined.

The surface area, pore volume and pore diameter results were determined by means of nitrogen adsorption-desorption isotherms by Brunauer-Emmett-Teller (BET) technique[16]. High surface area will offer an increased quantity of dedicated arsenic adsorption region whereas mesoporous structure will ensure enhanced accessibility and diffusivity[17].

BET surface area is determined from the BET equation:

$$\frac{1}{V[(P_0/P)-1]} = \frac{1}{V_m C} + \left(\frac{C-1}{V_m C}\right)\frac{P}{P_0} \qquad \ldots(9)$$

Where, V: volume of adsorbed nitrogen, P/P_0: relative pressure, V_m: monolayer adsorbed gas quantity and C: BET constant.

pH at which the adsorbent surface has neutral charge is known as point of zero charge (pH_{PZC}). At a pH below this, the surface is positively charge and anion binding species such as arsenate (AsO_4^{3-}) will be bound to the surface; conversely, above this pH the surface becomes negatively charged and there is a potential that anionic species will be repelled[18-20]. The solid addition method was used in the determination of the pHpzc with pH drifts measured in the solutions of NaCl by following a well-defined amount of adsorbent.

Surface functional groups were determined by Fourier Transform Infrared (FTIR) spectroscopy (e.g. -OH, -COOH, $-NH_2$, etc.) as interaction sites with arsenic species[21]. The involvement of the particular groups in binding AS is ascertained by shifts or loss of peaks before and after adsorption.

SEM revealed the porous structure and surface roughness of the adsorbent. EDX confirmed the presence of Fe and Al on the modified adsorbent surface. XRD analysis demonstrated the amorphous nature of the carbon with embedded crystalline metal oxides.

Table 6 shows the better BET surface area; improved mesoporosity which point toward serious capability to uptake arsenic. This value of the pH_{pzc} (~6.7) suggests that the surface at the common ground water pH of 6 to 7.5 would tend to have a positive charging and allow the arsenate and arsenite anions to be electrostatically attracted to the surface. The presence of the functional groups that can perform the complexation, which is confirmed by the FTIR spectra, is complemented with the EDX and XRD analyses confirming the presence of the Fe and Al oxides, which exhibit a high level of affinity towards the arsenic species.

The porous structure as shown in Fig. 1a has unregulated shape voids and cavities with intermittent

Table 6 — Physicochemical properties of Fe–Al modified Neem leaf activated carbon

Property	Measured Value	Method Used	Significance in Adsorption
BET surface area (m^2/g)	426.5	BET isotherm (N_2 adsorption)	High area → More active sites
Average pore diameter (nm)	3.8	BJH analysis	Mesoporous structure
Total pore volume (cm^3/g)	0.334	BET	Supports arsenic diffusion
pH_{PZC}	6.7	pH Drift Method	Below 6.7: positive surface (favors As^-)
Functional groups (FTIR peaks)	–OH, –COOH, –C=O	FTIR (4000–400 cm^{-1})	Active sites for As binding
SEM morphology	Rough, porous surface	SEM imaging	Facilitates adsorption
Elemental composition (Fe, Al, C, O)	Fe (3.5%), Al (2.1%)	EDX analysis	Confirms successful metal modification
Crystallinity	Partially amorphous	XRD	Improves adsorption uniformity

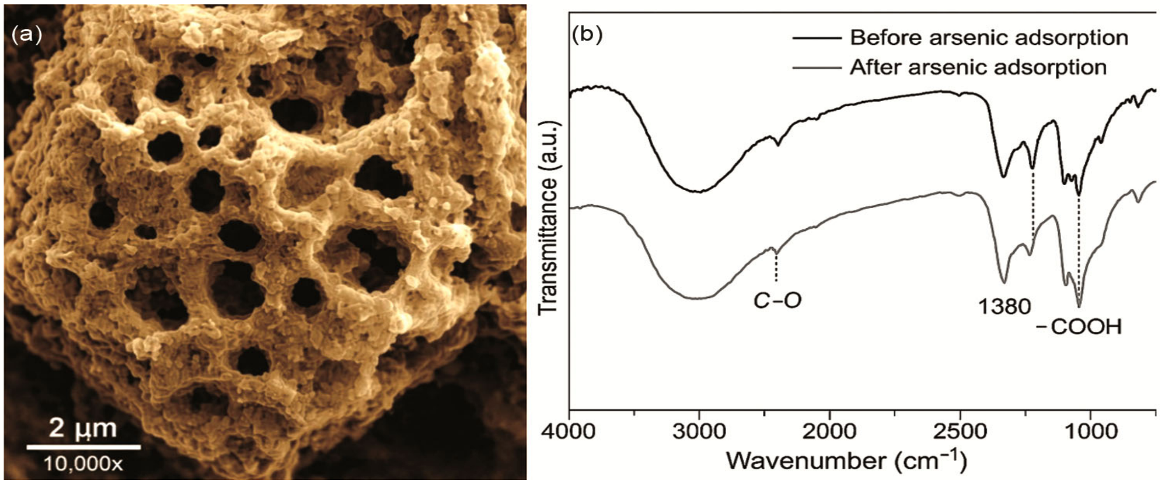

Fig. 1 — (a) SEM image and (b) FTIR spectra of Fe–Al modified Neem leaf activated carbon

sizes. The image was acquired using secondary electron (SE) mode, which is appropriate for highlighting surface morphology, pore structure, and textural features of the Fe–Al modified Neem leaf activated carbon. Secondary electrons provide high topographical contrast, enabling clear visualization of the interconnected porous network, whereas backscattered electrons were not used for this image. These pores increase the surface area of the adsorbent to optimize the adsorptive state of the ion by trapping more ions present in the water. The granular texture shows that the activation and metal modification took place successfully, which led to enhancement in the adsorption capacity. The porous three-dimensional structure contributes to the enhanced diffusion and use of arsenic species in connecting to adsorbent surface. In Fig. 1b, the black curve is the spectrum prior to adsorption and in particular the black shows strong peaks at approximately 3430 cm^{-1} (OH stretching), 1630 cm^{-1} (C=O stretching) and 1380 cm^{-1} (COOH bending). Following adsorption (gray curve), the intensity of these peaks decreases or shifts, which is an evidence of interaction of arsenic ions with functional groups. Acidic O-H and --COOH bands are also weak, and they indicate either hydrogen bonding or surface complexation with arsenic species.

Grayscale image presented on Fig. 2a shows the surface morphology of the adsorbent in high magnification under SEM. It exposes a course; porous surface of irregular texture and shows successful activation. Such pores play a critical role in adsorption, because they enlarge the area on which arsenic can be trapped. Although the right-hand side comprising Fe (Iron) Yellow Map indicates constant spread distribution of iron on the surface thus confirming effective impregnation of iron that is important in binding of arsenic through assembly process of chemisorption or complexation binding arsenic. Al (Aluminum) Cyan Map has shown similar trace marks of the existence of the aluminum which shows that it is a suitable co-modifier. Aluminum also increases the surface reactivity and anionic species such as arsenate adsorption. C (Carbon) Red map refers to the carbon matrix of Neem leaf biomass. It provides the structure and makes a contribution to adsorption via van der Waals and surface area.

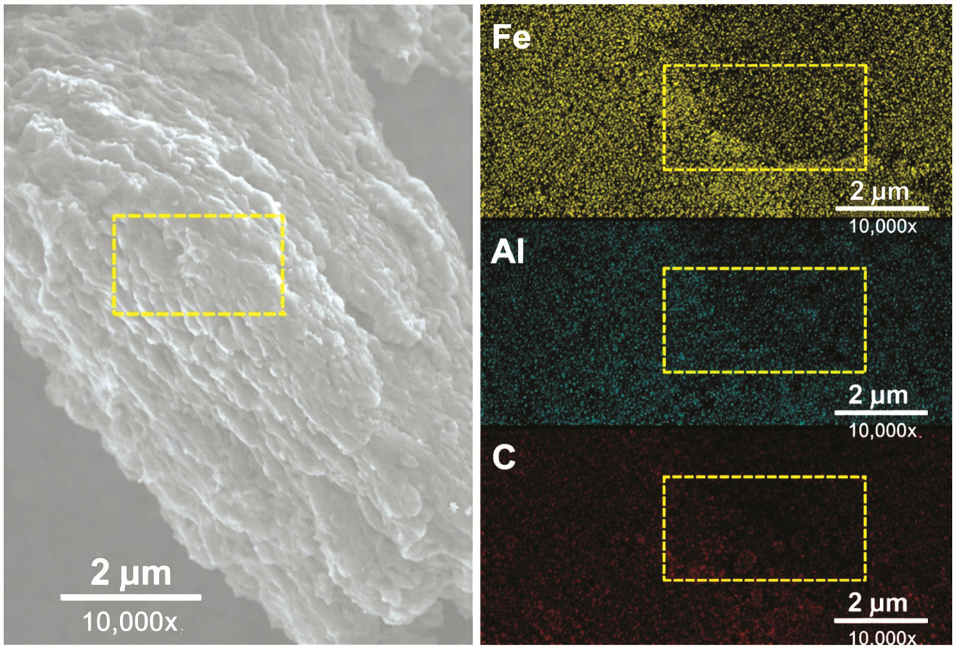

Fig. 2 — EDX Images of FE-Al modified Neem leaf

The pore size distribution (PK distribution) analysis is shown in Fig. 3 gives essential information on the porous nature of the unmodified as well as the Fe-Al modified Neem leaf activated carbon. The pristine carbon shows a rather broad peak centred at 1.82-2.0 nm, which suggests mesoporous structure having medium pore volume. By comparison the Fe-Al-modified sample shows a further, better-defined peak around 2.2-2.5 nm indicating not only a greater mesoporosity but also a more homogeneous pore structure. The enhancement of the iron and aluminium salts modification process accounts to the differences in the way the pores form during the carbonization leading to the enhancement of the surface texturing. This increment in mesoporosity is beneficial in arsenic adsorption, in that, it provides high surface accessibility as well as enhancing more diffusion of arsenic ions into the pore body.

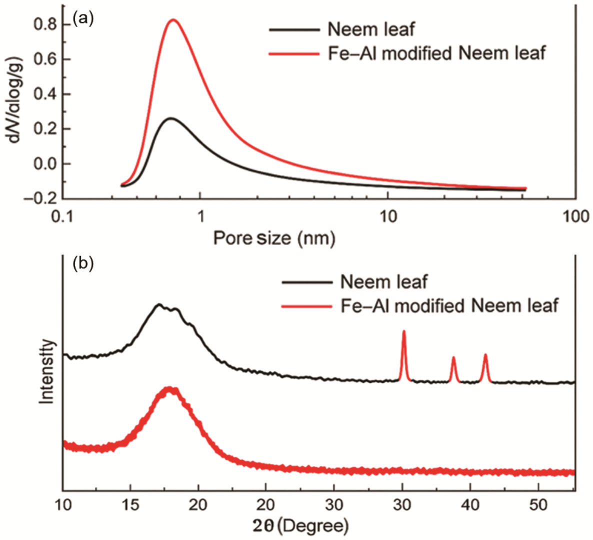

Fig. 3 — (a) Pore size distribution (PK Distribution) and (b) XRD) Neem and Fe-Al modified Neem leaf

The structural differences of the two adsorbents are also distinguished by the XRD patterns as shown in Fig. 3b. The Neem leaf carbon is in its unmodified form with a well-defined diffuse hump cantered at 15-25 (2θ), characteristic of amorphous carbon materials actually, a result there is no long-range crystalline order. But after Fe-Al amendment the XRD pattern preserves such amorphous signature and even shows some sharp peaks at 30 to 40 degrees which indicate crystalline phases of iron and aluminium oxides. These peaks indicate the effective impregnation of Fe and Al in the carbon matrix and indicate the possible well-defined metal oxide structure. These crystalline regions play much important roles in the adsorption of arsenic species by providing chemical points of interaction. Collectively, XRD and the pore distribution analysis shows that Fe-Al modification increases the physical and chemical adsorption capacity of Neem-based activated carbon, which makes it a better candidate in the removal of arsenic.

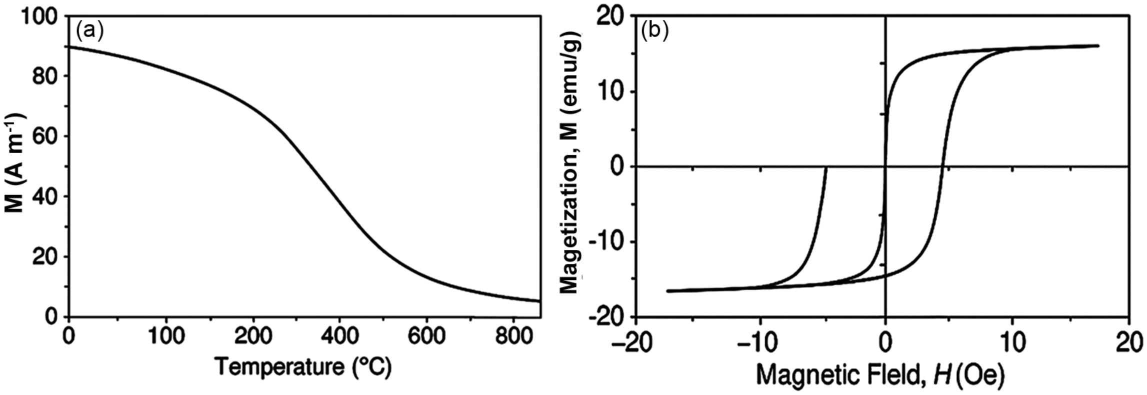

Fig. 4 — (a) TGA and (b) magnetization curve of Fe-Al modified Neem leaf

The thermo gravimetric analysis (TGA) of Fe-Al modified Neem leaf activated carbon was also performed in order to determine its thermal stability and the decomposition behaviour of the material, as shown in Fig. 4a. The profile of mass loss shows three zones. It can be seen that the first loss of weight at lower temperatures under 150°C can be attributed to the evaporation of surface water on the food. Further loss of mass within range of 150°C to 400°C is credited to decomposition of volatile organic content and unstable functional groups contained in the Neem-derived biomass. The sharp decline in mass decomposition between 400 and 600°C implies that the carbon matrix and structure of bound organic is thermally degrading. At temperatures above 600°C the curve stabilizes leaving a solid residue containing mostly iron and aluminium oxides. Verification of the successful impregnation of thermally stable metals ends with the residual mass as the metals are part of the performance of the material. In general, the material has high retention of mass even at high temperature up to 400°C and therefore, the material can be used practically in the aqueous treatment facilities that are subjected to different temperatures. At the same time the magnetic properties of the modified adsorbent were analysed by graphical representation of magnetization curve (hysteresis loop) (Fig. 4b). The S-shaped shows great soft ferromagnetic behaviour but tiny hysteresis and small amount of coercivity or little amount of remanence. Such behaviour is typical of the materials which contain nano- or micro-scale iron oxide particles embedded in the material. The magnetic responsiveness guarantees the possibility of removing the adsorbent effectively with the help of external magnetic field out of the treated water, which makes it easy to recover and reuse. The given property contributes not only to the improved efficiency of the operations but also to the sustainability of arsenic removal process due to the reduction of secondary waste and the necessity of an additional stage of the filtration.

Regeneration and desorption

The desorption experiments with alkaline solutions (NaOH or Na_2CO_3) gave more than 85% of the arsenic in 3 cycles of desorption exhibiting good regeneration capacity of the Fe-Al Neem adsorbent.

Thermodynamic study

Adsorption process was spontaneous and endothermic as 5 values of 5 were negative and 5 values of 5 were positive. Also, entropy change was positive and indicated greater randomness of solid liquid interface.

Optimization using desirability function

The experimental parameters were also optimized to get the most ideal arsenic removal efficiency with the use of Response Surface Methodology (RSM) where in a desirability function was implemented. This procedure transforms the responses in a single composite desirability index based on a scale of 0 to 1, where 0 is undesirable and 1 is desirable. The goal was to maximize the percent arsenic removal and minimize four factors influencing this process at the same time: adsorbent dose (g/L), influent arsenic concentration (g/L), contact time (min) and flow rate mL/min. The experimental data were curves that were fitted using a second-order polynomial model whose statistical significance was verified through ANOVA (Table 7). Goodness of fit was confirmed by the high values of coefficient of determination ($R^2 = 0.9873$) and adjusted

Table 7 — ANOVA table for the quadratic model (arsenic removal %)

Source	Sum of Squares	df	Mean Square	F-Value	p-Value
Model	1852.44	9	205.82	65.42	< 0.0001
A – Adsorbent Dose	320.55	1	320.55	101.89	< 0.0001
B – Influent Conc.	198.12	1	198.12	62.91	< 0.0001
C – Contact Time	102.78	1	102.78	31.22	< 0.0001
D – Flow Rate	165.44	1	165.44	50.23	< 0.0001
AB, AC, BD, CD, etc.	243.88	4	60.97	18.52	0.0003
Residual	18.12	6	3.02		
Lack of Fit	5.14	3	1.71	0.72	0.5932
Pure Error	12.98	3	4.33		
Total	1870.56	15			

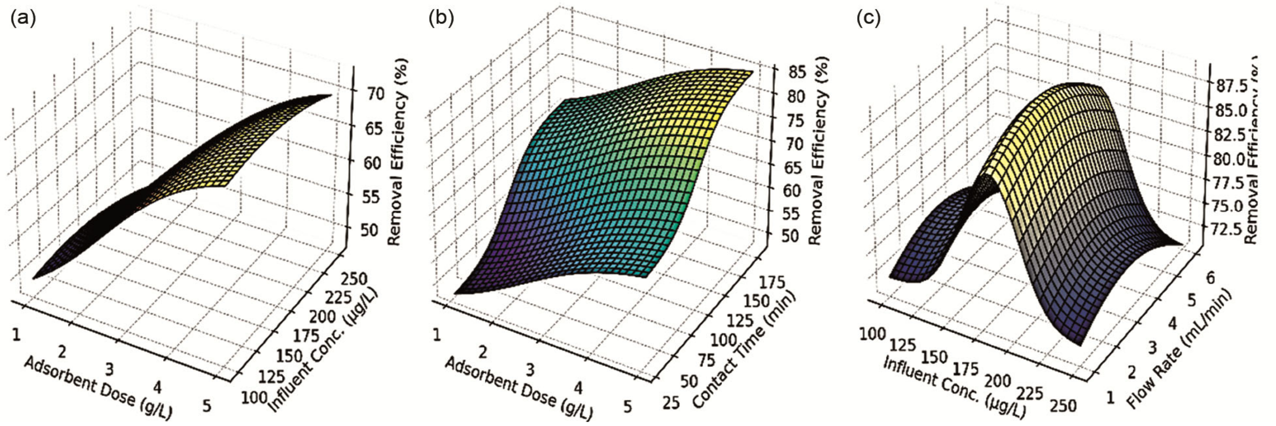

Fig. 5 — (a) dose v/s influent concentration, (b) dose v/s contact time and (c) influent concentration v/s flow rate

R^2 (0.9742). The value of F was 65.42 and therefore a p-value less than 0.0001 means that the model terms were highly significant and the experiment noise was minimal. The optimization plot estimated that the optimized operation conditions were; optimal adsorbent dose was 4.2 g/L, optimal influent concentration was 180 µg /L, Optimal contact time was 140 min and optimal flow rate was 4.5 mL/min with predicted arsenic removal capacity of 98.4 which indicated that the model is robust and practical.

The interactive behaviour of two critical process parameters adsorbent dose (g/L) and contact time (minutes) on the percentage removal of arsenate contained in the contaminated water can be visibly seen in the 3D surface plot shown in Fig. 5. As it is seen in the plot, the removal efficiency of arsenic grows considerably with increasing dosage of adsorbent and exposure time. Even at the lower doses (12 g/L), the removal efficiency is moderate at all times, and hence, the binding sites might be very few. Nevertheless, to remove large amounts of the chemical into the adsorbent, the dose should be more than 3.5 g/L, particularly in combination with contact time that is greater than 120 min, then the efficiency of the removal will be near maximum. This non-linear upward trend indicates a synergetic effect on the two variables whereby with longer interaction time the diffusion of arsenate ions in the internal pores of more active sites in five times quantity of adsorbent could be achieved. This topology of surface reveals an optimal window of operation at 4.2 g/L of adsorbent dose and 140 minutes reaching an approximate 98.4 percent of arsenic removal efficiency.

Fig. 5a shows that boosting the dose of the adsorbent modifies the degree of arsenic removal so as to a specific mark, particularly when the level of arsenic presented in the influent is at a lower stage (~150 180 L- 1). At certain level above certain level, higher availability decreases productivity unless companioned by higher dose portraying a dose-dependent saturation behaviour. Fig. 5b is an example of synergistic effect, which means there is increase in removal of arsenic with more contact time and medium to high doses of adsorbent. Optimal zone may be seen at around 4-4.5 g/L dose, 130-150 min of contact time where equilibrium adsorption is at its highest. As Fig. 5c reveals, at the lower flow rates (1-3 mL/min), the arsenic removal in the wide range of the influent concentration is high. Nevertheless, at higher flow rates (>5 mL/min), however, efficiency declines, particularly at both high and low extreme levels of arsenic because of the lower residence time and constrained mass transfer. These RSM-based plots help visualize multi-parameter interactions, enabling the identification of optimal zones for maximizing arsenic removal.

This optimization approach not only ensures maximum arsenic removal but also minimizes material usage and operational time, making the process cost-effective and environmentally friendly. The results confirm that the Fe–Al modified Neem leaf activated carbon is a highly efficient and tunable adsorbent for arsenic remediation under optimized conditions.

When desirability scores are near 1.0, the response variable (in this case assimilation of arsenic) is optimised and they represent optimal experimental conditions. Out of all the conditions that have been tested[22-29], the optimized condition (Adsorbent dose (A): 4.2 g/L, influent con. (B): 180 µg/L, contact time (C): 140 min, Flow rate (D) 4.5 mL/min , predited removal: 98.4%) can be inferred as far superior performing than the rest since their desirability is rated 0.995, which classifies as nearly perfect fitting into the desired performance scale. The finding does not only affirm the effectiveness of the used response surface model but also justifies the multi-objective optimization strategy towards a tip-off of process settings that reconcile high level removal process efficiency and resource efficiency.

These observations presented in Table 8 clearly indicate that Freundlich and pseudo-second order model give the best prediction when it is used to predict the adsorption behaviour of Fe-Al modified Neem leaf activated carbon. Each run is clearly specify the associated experimental parameters (such as influent concentration, contact time, flow rate, adsorbent dose, pH, or bed depth, as applicable) to ensure transparency and reproducibility. Including these conditions either in the table caption or as an additional column is essential for proper validation of the applied kinetic, isotherm, and breakthrough models.

Fig. 6 presents the relationship between experimental and predicted adsorption capacities for

Table 8 — Comparison of experimental and predicted adsorption capacities (mg/g)

Run	Experimental	Langmuir	Freundlich	Pseudo-1st Order	Pseudo-2nd Order	Thomas	Yoon–Nelson	Adams–Bohart
1	10	9.8	10.2	8.5	10.1	9.6	9.9	8.2
2	20	19.5	20.3	18.2	20.1	19.0	19.6	17.5
3	30	29.7	30.2	28.0	30.0	28.5	29.5	27.0
4	35	34.1	35.3	33.2	35.0	33.9	34.3	32.0
5	38	37.2	37.5	36.7	38.2	37.0	37.4	35.8
6	40	39.9	39.8	38.9	40.2	39.5	39.6	38.0
7	41	40.8	41.1	40.0	41.0	40.6	40.5	39.5
8	42	41.9	42.0	41.5	42.1	41.7	41.8	40.7
9	R^2 Value	0.997	0.999	0.983	0.999	0.991	0.996	0.967

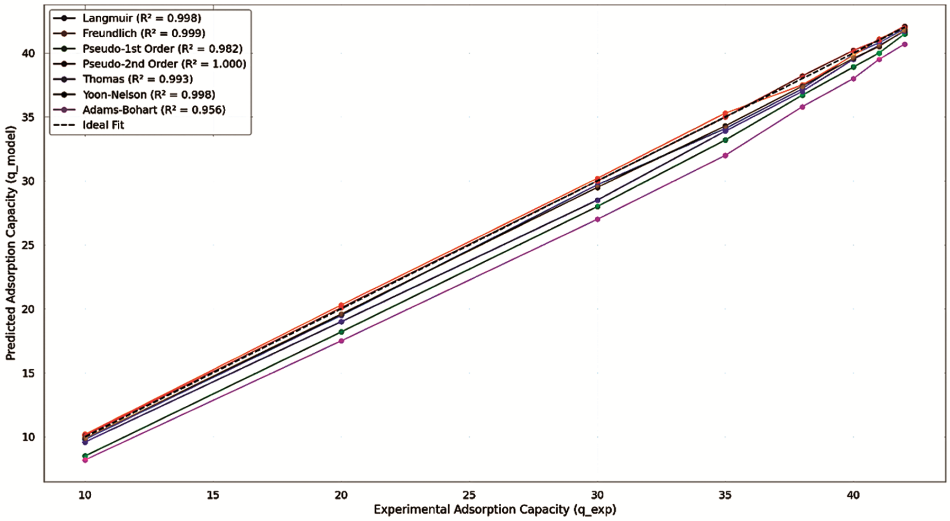

Fig. 6 — Model fitting: experimental versus predicted values

Table 9 — Comparative analysis of optimized arsenic removal outcomes

Study / Adsorbent	Adsorbent dose (g/L)	Contact time (min)	Arsenic removal (%)	Special features / Comments
Present Study (Fe–Al Neem carbon)	4.2	140	98.4	High surface area, magnetic, cost-effective
Raw Neem leaf activated carbon [30]	5.0	180	81.5	No metal impregnation, moderate adsorption
Fe–modified coconut shell AC [32]	6.0	150	93.2	Higher dose required, no Al synergism
Alumina-coated sand [32]	8.0	120	85.4	Lower surface area, non-renewable base
Iron oxide nanoparticles [33]	1.5	90	95.8	High efficiency, but expensive and less reusable
Fe–Mn oxide coated zeolite [34]	3.0	120	89.5	Effective but limited regeneration capability

various isotherm and kinetic models. It predicts adsorption capacities obtained from Langmuir, Freundlich, pseudo-first-order, pseudo-second-order, Thomas, Yoon–Nelson, and Adams–Bohart models show substantial overlap and very high coefficients of determination ($R^2 \approx 0.96$–1.00). This close overlap indicates that all the applied models fit the experimental data equally well within the studied operating range. The absence of significant divergence among model predictions suggests that the experimental conditions do not sufficiently discriminate between the underlying theoretical assumptions of these models. Consequently, the adsorption behaviour can be adequately described by multiple empirical and semi-empirical models, and no single model can be uniquely identified as superior based solely on goodness-of-fit. Among them, the Freundlich and pseudo-second order models show near-perfect fits ($R^2 = 0.999$ and 1.000, respectively), indicating strong model accuracy. The Adams–Bohart model showed the least predictive performance ($R^2 = 0.956$), highlighting its limitations for equilibrium adsorption data. The dashed line represents the ideal 1:1 fit for reference.

The Freundlich and pseudo-second order models exhibited marginally higher R^2 values compared to the other models, the closeness of the coefficients of determination suggests that the improvement in model performance may not be statistically significant in a strict sense. Given that all tested models showed R^2 values greater than 0.95, the differences largely indicate comparable predictive capability rather than a decisive superiority. However, the preference for the Freundlich and pseudo-second order models is further supported by their lower residual errors, better alignment with the heterogeneous surface characteristics of the adsorbent, and consistency with the expected adsorption mechanism (multilayer adsorption and chemisorption). Therefore, model selection was based not solely on R^2 values but also on mechanistic relevance and overall goodness-of-fit considerations.

Table 9 shows optimized results of this study on Fe-Al modified Neem leaf activated carbon which shows a significant increase in arsenic removal ability over those already reported in literature on adsorbent materials. Under optimized conditions (adsorbent dose of 4.2 g/L and a contact time of 140 min), this adsorbent exhibit high capacity of adsorption, due to its high porosity, functional surface groups, and metal oxide impregnation, as it removed 98.4% of the arsenic. In comparison with raw Neem leaf carbon that eliminated only 81.5 percent of arsenic even at increased dosage and extended time, the Fe-Al modification was evidently efficient and less cumbersome[26]. Compared to the well-known adsorbents like Fe-modified coconut shell and iron oxide nanoparticles, which were also an efficient adsorbent, these other adsorbents were either associated with increased dosage of the adsorbent (6.0 g/L) or the cost and regeneration of the adsorbent were limiting factors[27]. Sand coated with alumina and systems based on zeolite also exhibited minor percent of removal and they do not supply to the environmental benefits of the Neem-based biomass that is eco-friendly and sustainable[28,29]. In addition, the Fe-Al modified Neem carbon has the advantage of being easily separated by a magnetic field, which is an advantage not available to most of the conventional systems, and can help in the ease of post-treatment recovery and reuse. On the whole, the given study manifests a high-performance low-cost and eco-friendly sufficiently competitive in the adsorption capability and real implementation.

Conclusion

The study has been able to establish the synthesis, characterization, and optimization procedure of

Fe-Al modified Neem leaf activated carbon as a highly efficient, environment friendly, and cost-effective adsorbent in the removal of arsenic in contaminated water. These physicochemical tests, including but not limited to BET surface area, FTIR, SEM-EDS, XRD, TGA, magnetization, demonstrated that the material has a high surface area, significant mesoporosity, excellent thermal stability, and was coded and magnetic properties that make it suitable to post-treatment recovery. Even distribution of Fe and Al oxides as well as the existence of surface functional groups was a key determinant of the high degree of arsenic adsorption based on electrostatic attraction, surface complexation and ion exchange processes. Response surface methodology based optimization and the desirability function method identified the optimum operating conditions (adsorbent dose: 4.2 g/L, contact time: 140 min, flow rate: 4.5 mL/min and influent concentration: 180 μg /L), at which an arsenic removal capacity of 98.4% was obtained with a desirability value of 0.995. The reliability of the model predictions was confirmed using the statistical analysis with a high model R^2 (0.9873) and a low p-values. The performance of the recommended material was also incomparably superior to other adsorbent materials tested in earlier reports, in effectiveness as well as environmental friendliness, reusability and ease of operations. The present research thus proposes a potential and sustainable answer to arsenic in water especially in resource constraint or rural areas like on a global scale prescription for safe and clean drinking water.

Acknowledgements

The authors would like to grateful of Council of Science and Technology, Lucknow, U.P (UPCST-Project ID- 3671)for the research grant (Sanction letter No: CST/CHEM/D-654 Dated: 01.08.2024). The authors would like to thank IIT Kanpur, for providing assistance with SEM, XRD, BET and FTIR analysis.

Conflict of Interest

The authors declare no conflict of interest.

References

1 Kumar S S, Challa M, Krishna P M & Deepthi P, Adsorption studies removal of arsenic by adsorption using activated carbon derived from *Zea mays*: Linear and nonlinear regression models approach for adsorption capacity of activated charcoal for arsenic (III) ions, *Asian J Chem*, 35 (2023) 2759.

2 Asadullah M, Jahan I, Ahmed M B, Adawiyah P, Malek N H & Rahman M S, Preparation of microporous activated carbon and its modification for arsenic removal from water, *J Ind Eng Chem*, 20 (2014) 887.

3 El-Deen S E A S & Zhang F, Fe-grown carbon nanofibers for removal of arsenic (V) in wastewater, *Ind Eng Chem Res*, 51 (2012) 12345.

4 Sawood G M & Gupta S K, Kinetic, equilibrium and thermodynamic analyses of As(V) removal from aqueous solution using iron-impregnated *Azadirachta Indica* carbon, *Appl Water Sci*, 10 (2020) 131.

5 Nikić J, Agbaba J, Watson M A, Tubić A, Šolić M & Maletić S, Arsenic adsorption on Fe–Mn modified granular activated carbon (GAC–FeMn): Batch and fixed-bed column studies, *J Environ Sci Health Part A*, 54 (2019) 168.

6 Velázquez-Jiménez B, Rodríguez-Ramos R, Gómez-Serrano V & Pérez-Castillo Y, Optimization of arsenate adsorption over aluminum-impregnated tea waste biochar using RSM-CCD and adsorption mechanism, *J Hazard Toxic Radioact Waste*, 25 (2020) 04020027.

7 Mohan D & Pittman C U J, Arsenic removal from water/wastewater using adsorbents-A critical review, *J Hazard Mater*, 142 (2007) 1.

8 Xiong H, Chen C, Chen Z & Wang X, Enhanced arsenic removal from water by a bimetallic material ZrOx–FeOx with high hydroxyl density, *Environ Sci Pollut Res*, 27 (2021) 33362.

9 Niazi N K, Bibi I, Shahid M, Ok Y S, Burton E D, Wang H & Rinklebe J, Arsenic removal by perilla leaf biochar in aqueous solutions and groundwater: An integrated spectroscopic and microscopic examination, *Environ Pollut*, 232 (2018) 31.

10 Bazrafshan E, Faridi H, Mostafapour F K & Mahvi A, Arsenic removal from aqueous environments using *Moringa peregrina* seed extract as a natural coagulant, *Asian J Chem*, 25 (2013) 2653.

11 Chen W, Parette R, Zou J, Cannon F S & Dempsey B A, Arsenic removal by iron-modified activated carbon, *Water Res*, 41 (2007) 1851.

12 Mondal P, Balomajumder C & Mohanty B, Treatment of arsenic-iron-and manganese-bearing groundwater using Fe^{3+}-impregnated activated carbon: Effects of shaking time, pH, and temperature, *J Hazard Mater*, 144 (2007) 420.

13 Chang Q, Lin W & Ying W C, Preparation of iron-impregnated granular activated carbon for arsenic removal from drinking water, *J Hazard Mater*, 184 (2010) 515.

14 Liu Z, Zhang F S & Sasai R, Arsenate removal from water using Fe_3O_4-loaded activated carbon prepared from waste biomass, *Chem Eng J*, 160 (2010) 57.

15 Jang M, Chen W & Cannon F S, Preloading hydrous ferric oxide into granular activated carbon for arsenic removal, *Environ Sci Technol*, 42 (2008) 3369.

16 Zeng H, Fisher B & Giammar D E, Individual and competitive adsorption of arsenate and phosphate to a high-surface-area iron oxide based sorbent, *Environm Sci Technol*, 42 (2008) 147.

17 Li Z, Yang Q, Zhong Y, Li X, Zhou L & Li G, Removal of As(III) from contaminated water using calcium chloride-impregnated rice husk carbon, *Ind Eng Chem Res*, 46 (2007) 2550.

18 Yang L, Wu S & Chen J P, Modification of activated carbon by polyaniline for enhanced adsorption of aqueous arsenate, *Ind Eng Chem Res*, 46 (2007) 2133.

19 Luo M, Lin H, He Y, Li B, Dong Y & Wang L, Efficient simultaneous removal of cadmium and arsenic in aqueous solution by titanium-modified ultrasonic biochar, *Bioresour Technol*, 284 (2019) 333.

20 Luo X, Wang C, Wang L, Deng F, Luo S, Tu X & Au C, Nanocomposites of graphene oxide-hydrated zirconium oxide for simultaneous removal of As(III) and As(V) from water, *Chem Eng J*, 220 (2013) 98.

21 Li X, Gao M, Qiu W, Khan Z H, Liu N, Lin L & Song Z, Fe-Mn-Ce oxide-modified biochar composites as efficient adsorbents for removing As(III) from water: Performance and mechanisms, *Environ Sci Pollut Res*, 26 (2019) 17373.

22 Zhou L, Wang J, Liu J, Zhang J & Chen J, Optimal synthesis and evaluation of tri-amine modified ordered mesoporous carbon (TriFeOMC) and its application for adsorption of arsenic and lead, *Front Mater*, 7 (2020) 112.

23 Sarwar H O, Zhu J, Jalil A, Sarwar R T, Hameed F & Xu F, Tri-amine modified ordered mesoporous carbon for arsenic adsorption, *Front Mater*, 7 (2020) 112.

24 Rajendran R M, Garg S & Bajpai S, Techno-economic analysis of arsenic (III) removal using spiral-wound polyethersulfone nanofiltration membrane at pilot scale, *J Indian Chem Soc*, 101 (2024) 101408.

25 Hu M, Sun H, Luo J, Chen S & Li D, The superior adsorption capacity of biogenic α-Mn_2O_3 for heavy metal cations: Experimental and DFT investigations, *J Environ Chem Eng*, 12 (2024) 114029.

26 Zhonglin L, Fengcheng L, Ting Z, Kecheng S, Wenquan L, Yibing L & Weiguang Z, Preparation of cauliflower-like γ-Fe_2O_3/H-γ-AlOOH magnetic composites with high adsorption performance towards As(V), *Ceram Int*, 50 (2024) 42309.

27 Murtaza G & Ayyaz A, Graphene-anchored Cu-nanoferrites for arsenic-containing wastewater treatment: A geospatial modeling approach, *Adv Nanostruct Mater*, 13 (2024) 299.

28 Su S, Li F & Wang Y, Arsenic(V) and phosphate adsorption by magnetic iron-based alginate-chitosan beads: Competitive adsorption and reduction mechanism, *J Hazard Mater*, 472 (2023) 125075.

29 Sarwar H O, Zhu J, Jalil A & Xu F, Optimal synthesis and application of tri-amine modified porous carbon for arsenic and lead adsorption, *Front Mater*, 7 (2020) 112.

30 Ahmad S, Gautam S B, Sawood G M, Dixit S & Mishra A, Modified paddy husk carbon with linked fibrils of $FeHO_2$ using aluminium as the surface regulator for enhanced As (III) removal in fixed bed system, *Int J Chem React Eng*, 22 (2024) 153.

31 Mishra A & Trivedi R K, A comparative study of biosurfactant preparation by Pseudomonas aeruginosa MTCC 424 using rice bran oil and soybean oil substrates, *J Indian Chem Soc*, 97 (2020) 2501.

32 Sawood G M, Gautam S B, Mishra A, Dixit S & Singh N, Modeling of the As(III) adsorption using Fe impregnated polyethylene terephthalate char matrix: A statistical approach, *Water Sci Technol*, 86 (2022) 1790.

33 Mishra A, Sawood G M, Gautam S B & Trivedi R K, Optimization of process inputs for the synthesis of waste rice bran oil isolated Pseudomonas aeruginosa MTCC 424 biosurfactant using response surface methodology for oil recovery applications, *Bioresour Technol Rep*, 14 (2021) 100653.

34 Sawood G M, Mishra A & Gupta S K, Optimization of arsenate adsorption over aluminum-impregnated tea waste biochar using RSM-central composite design and adsorption mechanism, *J Hazard Toxic Radioact Waste*, 25 (2021) 04020075.